

Uncertainty through Polynomial Chaos in the EEG Problem

Rob H. De Staelen

Abstract—A sensitivity and correlation analysis of EEG sensors influenced by uncertain conductivity is conducted. We assume a three layer spherical head model with different and random layer conductivities. This randomness is modeled by Polynomial Chaos (PC). On average, we observe the least influenced electrodes along the great longitudinal fissure. Also, sensors located closer to a dipole source, are of greater influence to a change in conductivity – this is in agreement with previous research. The highly influenced sensors were on average located temporal. This was also the case in the correlation analysis, which was made possible by our approach with PC. Sensors in the temporal parts of the brain are highly correlated. Whereas the sensors in the occipital and lower frontal region, though they are close together, are not so highly correlated as in the temporal regions.

Index Terms—Polynomial Chaos, Electroencephalography, Uncertain conductivity, Sensitivity analysis, Correlation analysis.

I. INTRODUCTION

ELECTROENCEPHALOGRAPHY (EEG) is one of the most influential tools in the diagnosis of epilepsy and seizures, as it provides a record of ongoing electrical activity in the brain [1], [2]. The electrodes, connected to the EEG machine, measure signals produced by electrical discharge of neurons in the brain. The quasi-static approximation of the Maxwell equations is justified by the very low frequencies (typically < 100 Hz) involved. The total electric current \mathbf{J} can be partitioned [3] into two flows: a primary (driving) current \mathbf{J}^p related to neural sources, and an ohmic volume (passive) current \mathbf{J}^v that results from the effect of the electric field in the volume: $\mathbf{J} = \mathbf{J}^p + \mathbf{J}^v = \mathbf{J}^p + \sigma \mathbf{E} = \mathbf{J}^p - \sigma \nabla V$, where V is the electric potential. Since the total current is divergence free and no current flows outside the head, we obtain

$$\nabla \cdot (\sigma(\mathbf{r}) \nabla V(\mathbf{r})) = \nabla \cdot \mathbf{J}^p(\mathbf{r}), \quad \text{in } H \quad (1)$$

$$\boldsymbol{\nu} \cdot \sigma(\mathbf{r}) \nabla V(\mathbf{r}) = 0, \quad \text{on } \partial H \quad (2)$$

where H is the head, σ the conductivity and $\boldsymbol{\nu}$ the outward unit normal on ∂H .

A. Model assumptions

Usually, the head is assumed to be made up of disjoint layered regions (the scalp, skull, cerebrospinal fluid, grey matter and white matter, etc.) in each of which the conductivity is constant. We will use a *spherical head model* with three layers: the inner sphere (radius .87) represents the brain, the intermediate layer (radius .92) represents the skull and the outer sphere (radius 1) corresponds to the scalp, see Fig.

1(b). The outer and inner layer are assumed to have similar electrical properties, meaning that $\sigma_{\text{scalp}} = \sigma_{\text{brain}}$. Although we only consider a fixed (spherical) geometry, more realistic models exist and the effect of choice has been studied [4].

A widely used approximation of the neural activity of patients suffering from epilepsy [5] is the representation of the primary current as an electric dipole with dipole moment \mathbf{d} located at \mathbf{r}_d inside the cortex; $\mathbf{J}^p(\mathbf{r}) = \mathbf{d} \delta(\mathbf{r} - \mathbf{r}_d)$ with \mathbf{r} the position in the head measured from the center of the concentric spheres and δ the Dirac measure. It is clear that the sensitivity and correlation of the electrodes is key for a full understanding of EEG measurements.

B. Aim and novelty

The conductivity is in fact not constant in each layer and determining the conductivity values in the human head has been subject of research since many years [6]. Instead of working with the two different conductivities σ_{skull} and σ_{brain} , we consider the *conductivity ratio* $X = \sigma_{\text{skull}}/\sigma_{\text{brain}}$. Based on in vivo measurements [7] we assume it to be uniformly distributed with mean .026 and standard deviation of .0092. Some authors use a Gamma distributed conductivity ratio, this incorporates more a priori knowledge. Instead, we use the most uninformative distribution, thus reflecting the least a priori knowledge about the conductivity ratio.

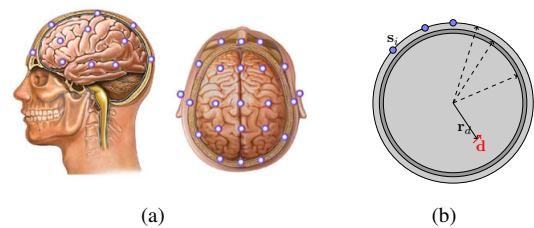


Figure 1. A standard 27 electrode placement (a) and a spherical head illustration (b) with sensors s_i .

We want to investigate the influence of this uncertainty on the sensitivity of EEG sensor measurements at sensor locations s_i . To this end, we will employ *Polynomial Chaos*. Previous studies use statistical error measures [8], the relative difference measure (RDM) [9], analysis of variance with related Cramér-Rao bound [10], etc. In Fig. 1(a) a standard 27 electrode placement is shown. Polynomial Chaos has the advantage that each sensor is represented as a single random variable, directly relating to the uncertain input.

This representation has another benefit. We can investigate the correlation between sensors very effectively. Since the 27 sensors are random variables, correlation is investigated through the correlation function of random variables. Though noise correlations and heteroscedasticity across sensors [11],

Manuscript received November 19, 2010; revised January 17, 2011.

R. De Staelen is with the Research Group of Numerical Analysis and Mathematical Modeling at the Department of Mathematical Analysis, Ghent University, B-9000 Ghent, Belgium (e-mail: Rob.DeStaelen@UGent.be).

[12] has been investigated, to our knowledge no studies about intrinsic EEG sensor correlation exist.

To (partially) validate our technique we compare our results with recent studies [9], [13], [14] about the fact that the location and orientation of the dipole source is one factor influencing the sensitivity: for the same electrode placement, sensitivity is maximum to dipole sources oriented parallel to the line of the electrodes regardless of source location.

II. METHODS

A. The EEG lead field model

To calculate the potential at the 27 sensor locations \mathbf{s}_i one needs to solve system (1)-(2) for V and evaluate $S_i = V(\mathbf{s}_i)$. Analytic solutions exist only for special cases [15]; in general the system of equations has to be solved numerically. The most prominent technique is the boundary element method (BEM). Instead of directly solving for the electric potential induced by a current dipole (e.g. through BEM), one can solve for the electric *lead fields* [16]. Invoking this method, the sensor measurements are given by

$$\mathbf{S} = \mathbf{L}(\mathbf{r}_d, X)\mathbf{d}, \quad \mathbf{S} = (S_i)_{i=1}^{27},$$

where $\mathbf{L} \in \mathbb{R}^{27 \times 3}$ is the *lead field* matrix which depends only on the dipole position, conductivity ratio, and the geometry.

We turn to the modeling of the uncertain conductivity ratio.

B. Polynomial Chaos expansion

Consider a probability space $(\Omega, \mathcal{F}, \mathbb{P})$ where Ω is the sample space, $\mathcal{F} \subseteq 2^\Omega$ a σ -algebra and \mathbb{P} a measure. The Hilbert space of random variables $Y : \Omega \rightarrow \mathbb{R}$, for which $\mathbb{E}[Y^2] < +\infty$ is denoted $\mathcal{L}^2(\Omega, \mathcal{F}, \mathbb{P})$. The space $\mathcal{L}^2(\Omega, \mathcal{F}, \mathbb{P})$ can be decomposed [17] into orthogonal spaces of polynomials with a random argument. According to this result (and its generalizations [18]) a random variable Y can be represented as a truncated series expansion

$$Y(\omega) = \sum_{i=0}^{\overline{n,p}} a_i \Psi_i(\boldsymbol{\xi}(\omega)), \quad \overline{n,p} + 1 = \binom{n+p}{p},$$

where $\boldsymbol{\xi} = (\xi_1, \dots, \xi_n)$ is a vector of i.i.d. random variables, $\{\Psi_i\}_{i \in \mathbb{N}}$ a family of orthogonal polynomials (expansion basis) and p is the chaos order. When $n = 1$ then $p = 3$ is usually sufficient. Since $\mathbb{E}[\Psi_i(\boldsymbol{\xi})\Psi_j(\boldsymbol{\xi})] = \delta_{ij}$, the expansion coefficients are given by $a_i = \mathbb{E}[Y\Psi_i(\boldsymbol{\xi})]$. Depending on the type of random input variable Y an optimal (in the sense of convergence rate) expansion basis can be found. This expansion is in general referred to as the Wiener-Askey Polynomial Chaos since the basis polynomials are these from the *Askey-scheme* of the hypergeometric functions. E.g., Hermite polynomials correspond to a Gaussian variable and the Legendre polynomials correspond to a uniform variable.

C. Uncertainty propagation

We assume all input is stochastic. This means the conductivity ratio as well as the moment and location of the dipole are modeled by random variables. As assumed in the Introduction, the uncertainty is uniform, so we employ Legendre Chaos. The conductivity ratio is then written as

$X(\xi_X) = .026 + .0159\xi_X$ where ξ_X is uniformly distributed on the interval $[-1, 1]$. Likewise the position \mathbf{r}_d resp. moment \mathbf{d} are written in terms of uniform variables $\boldsymbol{\xi}_{\mathbf{r}_d} = (\xi_{r^a}, \xi_{\theta^a}, \xi_{\phi^a})$ resp. $\boldsymbol{\xi}_{\mathbf{d}} = (\xi_{r^d}, \xi_{\theta^d}, \xi_{\phi^d})$ and are confined to the inner sphere. By Doob-Dynkin's lemma the solution can be expressed in terms of $\boldsymbol{\xi} = (\boldsymbol{\xi}_{\mathbf{r}_d}, \boldsymbol{\xi}_{\mathbf{d}}, \xi_X)$. A Legendre Chaos of order p of the i -th sensor reads (with λ_j the j -th 7-variate Legendre polynomial)

$$S_i(\boldsymbol{\xi}) = \mathbf{L}(\mathbf{r}_d(\boldsymbol{\xi}_{\mathbf{r}_d}), X(\xi_X))\mathbf{d}(\boldsymbol{\xi}_{\mathbf{d}}) = \sum_{j=0}^{\overline{7,p}} V_{ij}\lambda_j(\boldsymbol{\xi}). \quad (3)$$

The coefficients $V_{ij} = \mathbb{E}[S_i(\boldsymbol{\xi})\lambda_j(\boldsymbol{\xi})] \in \mathbb{R}$ were computed through a regression method, in this context referred to as a *stochastic response surface*. Since we have $n = 7$ random dimensions, we consider a Legendre Chaos of order $p = 7$. The effect of increasing the order of the chaos expansion may be of interest, but for our purposes we verified that 7 suffices; $\overline{7,7} = 3431$.

III. RESULTS AND DISCUSSION

A. Sensitivity analysis

We will discuss the sensitivity analysis at three stages. However, first we construct some input to work with. We consider the stochastic position and moment vectors $\mathbf{r}_d(\boldsymbol{\xi}_{\mathbf{r}_d})$ and $\mathbf{d}(\boldsymbol{\xi}_{\mathbf{d}})$ evaluated at some fixed stochastic input vectors, namely

$$\begin{aligned} \mathbf{r}_d(-.7, .2, .43) &= (-.027, -.121, -.041) = \mathbf{r}_d^1, \\ \mathbf{r}_d(.6, -.8, -.2) &= (-.174, .126, .662) = \mathbf{r}_d^2, \\ \mathbf{d}(.05, -.1, .2) &= (-.365, -.265, .071). \end{aligned}$$

Note that \mathbf{r}_d^1 is rather (deep) central in the cortex ($|\mathbf{r}_d^1| = .13$) whereas \mathbf{r}_d^2 is (shallow) closer to the skull ($|\mathbf{r}_d^2| = .74$). Having computed the chaos coefficients, we obtain 27 random variables S_i . We do not know its probability distribution but can regard it as function of the random variable $\boldsymbol{\xi}$.

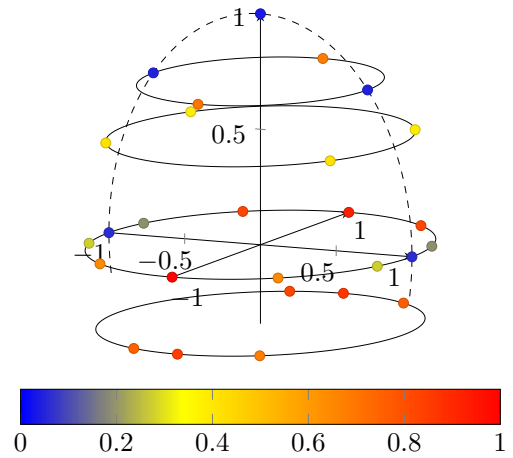


Figure 2. Normalized overall mean degree of influence $\bar{\kappa}$. The dashed line represents the great longitudinal fissure.

The *first stage* consists in marginalizing with respect to position and moment of the dipole to obtain the *overall mean*

sensorial response

$$\bar{\mathbf{S}}(\xi_X) = \mathbb{E}[\mathbf{S}(\xi) \mid \xi_X] = \frac{1}{2^6} \int_{-1}^1 \mathbf{S}(\xi) d\xi_{r_d} d\xi_d.$$

This relates the sensor measurements to the conductivity ratio with dipole location and moment averaged out. To quantify the sensitivity of sensor measurements with respect to a change in the conductivity ratio we define the *overall mean (relative) degree of influence* $\bar{\kappa}_i$ as

$$\bar{\kappa}_i = \frac{\bar{\kappa}'_i}{\sum_j \bar{\kappa}'_j}, \quad \bar{\kappa}'_i = \max_{|\xi_X| \leq 1} \bar{S}_i(\xi_X) - \min_{|\xi_X| \leq 1} \bar{S}_i(\xi_X),$$

for $i = 1, \dots, 27$. The results are shown in Fig. 3. Due to geometry arguments, we expect the overall mean influence to be symmetric with respect to the great longitudinal fissure. The overall mean degree of influence is normalized and the sensors are colored accordingly, see Fig. 2. Indeed we observe the expected symmetry and moreover the sensors located at the great longitudinal fissure are least influenced by a change in conductivity ratio. Note that Fig. 2 lacks a dipole, because there is averaged over location and moment; only geometry and conductivity play a role here.

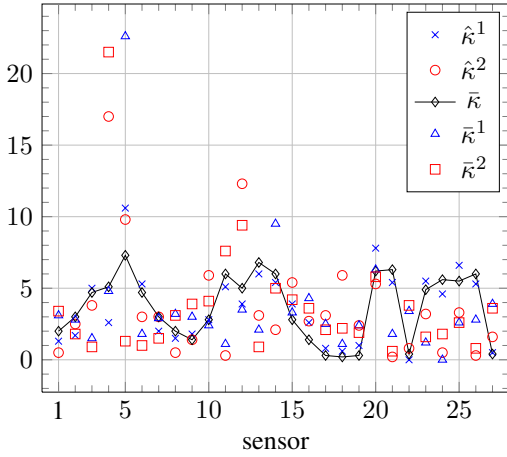


Figure 3. Different degrees of influence (in %) per sensor.

At the *second stage* we average out only the moment. This relates the sensor measurements to the conductivity ratio with fixed dipole location $\mathbf{r}_d^\ell = \mathbf{r}_d(\xi_{r_d}^\ell)$ but the moment averaged out. We define the *located mean sensorial response*

$$\bar{\mathbf{S}}^\ell(\xi_X) = \mathbb{E}[\mathbf{S}(\xi) \mid \xi_{r_d}^\ell, \xi_X] = \frac{1}{2^3} \int_{-1}^1 \mathbf{S}(\xi) d\xi_d,$$

with $\ell = 1, 2$. This enables us to quantify the influence of position regardless of orientation of the dipole source; we define the *located mean (relative) degree of influence* $\bar{\kappa}_i^\ell$ as

$$\bar{\kappa}_i^\ell = \frac{\bar{\kappa}'_i^\ell}{\sum_j \bar{\kappa}'_j^\ell}, \quad \bar{\kappa}'_i^\ell = \max_{|\xi_X| \leq 1} \bar{S}_i^\ell(\xi_X) - \min_{|\xi_X| \leq 1} \bar{S}_i^\ell(\xi_X),$$

for $i = 1, \dots, 27$ and $\ell = 1, 2$. Sensors located closer to the source, should have a greater influence w.r.t. a change in conductivity ratio. To verify these intuitive thought, we make a plot of the sensors in position with the sources shown as cubes, see Fig. 4. Our conjectures are indeed supported. Moreover they agree with previous results of [13], [19].

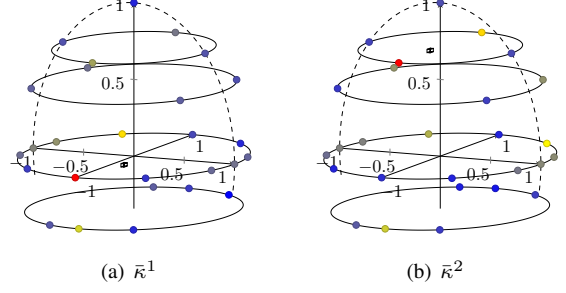


Figure 4. The normalized located mean degree of influence $\bar{\kappa}^{1,2}$ with the dipole positions $\mathbf{r}_d^{1,2}$ shown as cubes. The dashed line represents the great longitudinal fissure. (Same color coding as in Fig. 2.)

The *third stage* consists of no averaging. For an observed position and moment of the dipole source we denote the *observed sensorial response* as

$$\hat{\mathbf{S}}^\ell(\xi_X) = \mathbf{S}(\xi_{r_d}^\ell, .05, -.1, .2, \xi_X), \quad \ell = 1, 2,$$

according to the dipole location $\mathbf{r}_d^\ell = \mathbf{r}_d(\xi_{r_d}^\ell)$. As above, we define the *observed (relative) degree of influence* as

$$\hat{\kappa}_i^\ell = \frac{\hat{\kappa}'_i^\ell}{\sum_j \hat{\kappa}'_j^\ell}, \quad \hat{\kappa}'_i^\ell = \max_{|\xi_X| \leq 1} \hat{S}_i^\ell(\xi_X) - \min_{|\xi_X| \leq 1} \hat{S}_i^\ell(\xi_X),$$

for $i = 1, \dots, 27$ and $\ell = 1, 2$. The results are visualized in Fig. 3 and Fig. 5. Again we observe the location as an influential factor. But we note that the dipole orientation is fairly horizontal. When we consider a vertically oriented dipole, then we observe what is in line with what we already cited, namely: sensitivity is maximum to sources oriented parallel to the line of the electrodes [14].

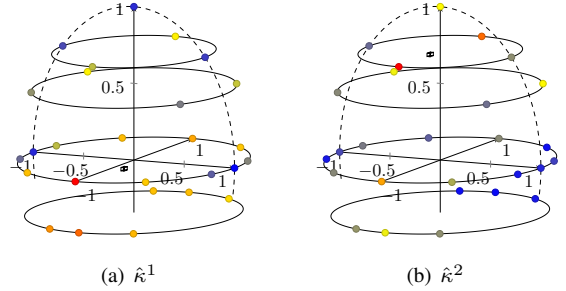


Figure 5. The normalized observed degree of influence $\hat{\kappa}^{1,2}$ with the dipole positions $\mathbf{r}_d^{1,2}$ shown as cubes. The dashed line represents the great longitudinal fissure. (Same color coding as in Fig. 2.)

B. Correlation analysis

It is reasonable to suspect some intrinsic correlation of EEG sensors, e.g. due to position. To quantify and investigate this we make use of our stochastic approach at hand. The correlation between sensor i and sensor j is $\rho_{ij} = \text{Corr}(S_i, S_j)$. This correlation is readily computed since we have a Legendre Chaos, which enables us to write the correlation in terms of the chaos expansion coefficients as

$$\rho_{ij} = \frac{\sum_{k=1}^{\bar{7},\bar{7}} V_{ik} V_{jk}}{\sqrt{\sum_{k=1}^{\bar{7},\bar{7}} V_{ik}^2} \sqrt{\sum_{k=1}^{\bar{7},\bar{7}} V_{jk}^2}}.$$

In Fig. 6 the sensors i and j are connected by a blue dashed line if $0 \leq |\rho_{ij}| < .02$, they are connected by a red solid line if $.9 \leq |\rho_{ij}| < 1$. We observe high correlations in the temporal region. It is apparent that the sensors in the occipital and lower frontal region, which are close together, are not so highly correlated as in the temporal regions. We note that we are dealing with overall mean sensor correlation, i.e. for averaged out dipole location, moment and conductivity ratio.

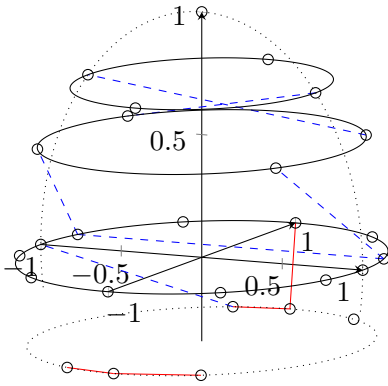


Figure 6. Visualization of correlation analysis. If $0 \leq |\rho_{ij}| < .02$ then sensor i is connected with sensor j by a blue dashed line. If $.9 \leq |\rho_{ij}| < 1$ then sensor i is connected with sensor j by a red solid line.

We remind that it were also these sensors that are on average most influenced by a change in the conductivity ratio, see Fig. 2. When solving the inverse problem – of locating a dipole when sensor measurements are at hand – one needs to take these results into account: temporal sensors are highly correlated and highly sensitive to the conductivity ratio. E.g., one can give them less weight or try to minimize their influence in the solution of the inverse problem. Ideally a real time sensitivity and correlation analysis is combined with the techniques used to address the inversion.

Explaining this results qualitatively is a next step, where expert medical judgement, physiological and anatomical expertise are required. This will be dealt with in the near future, being part of a interdisciplinary project.

IV. CONCLUSION

We discussed the modeling of the stochastic propagation of uncertain conductivity in EEG. Polynomial Chaos is introduced in the sensitivity and correlation analysis of the sensors influenced by uncertain conductivity. The analysis was conducted on a three layer spherical head model. We addressed the sensitivity analysis at three stages: dipole location and moment averaged out, only the dipole moment averaged out, and both fixed. On average, we observe the least influenced electrodes along the great longitudinal fissure. We compared two different source locations and obtained changes in the electrodes sensitivity, which we believe, are consistent with our intuitive hypothesis. The highly influenced sensors were on average located temporal. This was also the case in the correlation analysis. Sensors in the temporal parts of the brain are highly correlated. Whereas the sensors in the occipital

and lower frontal region, though they are close together, are not so highly correlated as in the temporal regions.

We hope this effective quantification of sensitivity and correlation can be useful in the EEG inverse problem, where iteratively the least influenced/correlated sensors are given more weight in the inverse algorithm. We are now trying to also make some sensor locations random and look for optimal placing of these sensors. Also, a more realistic head model and anisotropic conductivity distributions are a natural next topic of investigation [8].

Collaboration with researchers specifically dealing with practical EEG applications in medical investigations, will be set up in the frame of an interdisciplinary project between engineers, physicians and mathematicians. We continuously aim at contributing to the improvement of the reliability of the interpretation and use of the EEG-results in medical prognoses and remediation. We hope to report on this further research in a future WCE.

ACKNOWLEDGMENT

The author would like to thank the department of Electrical Energy, Systems and Automation (*EESA*) at Ghent University, and in particular Guillaume Crevecoeur, for providing the basis of a computer algorithm to compute the lead field. His office colleague Tine Goessens and colleague Hilde De Ridder are thanked for the fruitful discussions. His supervisors Roger Van Keer and Marián Slodička are thanked for their support.

REFERENCES

- [1] M. Nolan, M. Redoblado, S. Lah, M. Sabaz, J. Lawson, A. Cunningham, A. Bleasel, and A. Bye, "Memory function in childhood epilepsy syndromes," *Journal of Paediatrics and Child Health*, vol. 40, pp. 20–27(8), January 2004.
- [2] H. Urbach, "Imaging of the epilepsies," *European Radiology*, vol. 15, pp. 494–500, 2005.
- [3] M. Hämäläinen, R. Hari, R. Ilmoniemi, J. Knuutila, and O. V. Lounasmaa, "Magnetoencephalography—theory, instrumentation, and applications to noninvasive studies of the working human brain," *Rev. Mod. Phys.*, vol. 65, no. 2, pp. 413–497, Apr 1993.
- [4] N. von Ellenrieder, C. Muravchik, M. Wagner, and A. Nehorai, "Effect of head shape variations among individuals on the EEG/MEG forward and inverse problems," *Biomedical Engineering, IEEE Trans. on*, vol. 56, no. 3, pp. 587–597, mar. 2009.
- [5] J. de Munck, B. van Dijk, and H. Spekreijse, "Mathematical dipoles are adequate to describe realistic generators of human brain activity," *Biomedical Engineering, IEEE Trans. on*, vol. 35, no. 11, pp. 960–966, nov. 1988.
- [6] L. Geddes and L. Baker, "The specific resistance of biological material—A compendium of data for the biomedical engineer and physiologist," *Medical and Biological Engineering and Computing*, vol. 5, pp. 271–293, 1967.
- [7] S. Goncalve, J. de Munck, J. Verbunt, R. Heethaar, and F. da Silva, "In vivo measurement of the brain and skull resistivities using an EIT-based method and the combined analysis of SEF/SEP data," *Biomedical Engineering, IEEE Trans. on*, vol. 50, no. 9, pp. 1124–1127, sep. 2003.
- [8] C. Wolters, A. Anwander, X. Tricoche, D. Weinstein, M. Koch, and R. MacLeod, "Influence of tissue conductivity anisotropy on EEG/MEG field and return current computation in a realistic head model: A simulation and visualization study using high-resolution finite element modeling," *NeuroImage*, vol. 30, no. 3, pp. 813–826, 2006.
- [9] S. Vallaghe and M. Clerc, "A global sensitivity analysis of three- and four-layer EEG conductivity models," *Biomedical Engineering, IEEE Trans. on*, vol. 56, no. 4, pp. 988–995, apr. 2009.
- [10] S. Cavassila, S. Deval, C. Huegen, D. van Ormondt, and D. Graveron-Demilly, "Cramér-Rao bounds: an evaluation tool for quantitation," *NMR in Biomedicine*, vol. 14, pp. 278–283, 2001.

- [11] A. Dogandzic and A. Nehorai, "Estimating evoked dipole responses in unknown spatially correlated noise with EEG/MEG arrays," *Signal Processing, IEEE Trans. on*, vol. 48, no. 1, pp. 13–25, jan. 2000.
- [12] H. M. Huizenga and P. C. M. Molenaar, "Equivalent source estimation of scalp potential fields contaminated by heteroscedastic and correlated noise," *Brain Topography*, vol. 8, pp. 13–33, 1995.
- [13] N. Gencer and C. E. Acar, "Sensitivity of EEG and MEG measurements to tissue conductivity," *Physics in Medicine and Biology*, vol. 49, no. 5, p. 701, 2004.
- [14] S. Rush and D. Driscoll, "EEG electrode sensitivity - An application of reciprocity," *Biomedical Engineering, IEEE Trans. on*, vol. 16, no. 1, pp. 15–22, jan. 1969.
- [15] D. B. Geselowitz, "On bioelectric potentials in an inhomogeneous volume conductor," *Biophysical Journal*, vol. 7, no. 1, pp. 1–11, 1967.
- [16] J. Riera and M. Fuentes, "Electric lead field for a piecewise homogeneous volume conductor model of the head," *Biomedical Engineering, IEEE Trans. on*, vol. 45, no. 6, pp. 746–753, jun. 1998.
- [17] N. Wiener, "The homogeneous chaos," *American Journal of Mathematics*, vol. 60, no. 4, pp. 897–936, 1938.
- [18] D. Xiu and G. E. Karniadakis, "The Wiener-Askey Polynomial Chaos for stochastic differential equations," *SIAM J. Sci. Comput.*, vol. 24, no. 2, pp. 619–644, 2002.
- [19] J. Haueisen, C. Ramon, M. Eiselt, H. Brauer, and H. Nowak, "Influence of tissue resistivities on neuromagnetic fields and electric potentials studied with a finite element model of the head," *Biomedical Engineering, IEEE Trans. on*, vol. 44, no. 8, pp. 727–735, aug. 1997.